J Neurophysiol 104: 3180–3188, 2010.
First published October 6, 2010; doi:10.1152/jn.00574.2010.

Social and Ecological Regulation of a Decision-Making Circuit

H. Neumeister,[1,*] K. W. Whitaker,[2,3,*] H. A. Hofmann,[2,4,5,†] and T. Preuss[1,†]

[1]*Department of Psychology, Hunter College, City University of New York, New York;* [2]*Institute for Neuroscience,* [4]*Institute for Cellular and Molecular Biology, and* [5]*Section of Integrative Biology, The University of Texas at Austin, Austin, Texas; and* [3]*Army Research Laboratory, Aberdeen Proving Grounds, Maryland*

Submitted 28 June 2010; accepted in final form 1 October 2010

Neumeister H, Whitaker KW, Hofmann HA, Preuss T. Social and ecological regulation of a decision-making circuit. *J Neurophysiol* 104: 3180–3188, 2010. First published October 6, 2010; doi:10.1152/jn.00574.2010. Ecological context, sensory inputs, and the internal physiological state are all factors that need to be integrated for an animal to make appropriate behavioral decisions. However, these factors have rarely been studied in the same system. In the African cichlid fish *Astatotilapia burtoni*, males alternate between two phenotypes based on position in a social hierarchy. When dominant (DOM), fish display bright body coloration and a wealth of aggressive and reproductive behavioral patterns that make them conspicuous to predators. Subordinate (SUB) males, on the other hand, decrease predation risk by adopting cryptic coloration and schooling behavior. We therefore hypothesized that DOMs would show enhanced startle-escape responsiveness to compensate for their increased predation risk. Indeed, behavioral responses to sound clicks of various intensities showed a significantly higher mean startle rate in DOMs compared with SUBs. Electrophysiological recordings from the Mauthner cells (M-cells), the neurons triggering startle, were performed in anesthetized animals and showed larger synaptic responses to sound clicks in DOMs, consistent with the behavioral results. In addition, the inhibitory drive mediated by interneurons (passive hyperpolarizing potential [PHP] cells) presynaptic to the M-cell was significantly reduced in DOMs. Taken together, the results suggest that the likelihood for an escape to occur for a given auditory stimulus is higher in DOMs because of a more excitable M-cell. More broadly, this study provides an integrative explanation of an ecological and social trade-off at the level of an identifiable decision-making neural circuit.

INTRODUCTION

In many species, males signal social rank and breeding status through conspicuous coloration and behavioral displays (Dijkstra et al. 2007; Godin and Dugatkin 1996; Godin and McDonough 2003). The obvious benefit of these signals for resource acquisition and reproduction are often countered by ecological costs such as an increase in predation risk caused by the decrease in crypsis (Endler 1978, 1991; Godin and McDonough 2003; Huhta et al. 2003; Lyytinen et al. 2003; Maan et al. 2008; Pruden and Uetz 2004). Animals show adaptations to this life history trade-off by adjusting behavioral responsiveness to predators to compensate for the increased risk (Dill 1990; Godin and Dugatkin 1996; Martin and Lopez 1999; Ydenberg and Dill 1986). Therefore predator avoidance strategies may be adaptive depending on social rank and/or breeding state. This would require sensorimotor circuits that integrate both external stimuli and the individual's internal physiological state as determined by its social rank. Such interactions are common (Gilmour et al. 2005), but the underlying neural processes and computations remain unclear.

The African cichlid *Astatotilapia burtoni* is a powerful model system in social neuroscience (Fernald 2002; Hofmann 2003; Robinson et al. 2008; Wong and Hofmann 2010). In this species, males alternate between two socially dependent phenotypes throughout their lives. When an individual is dominant (DOM) in a social group, he maintains a territory, bright body coloration, and displays a vigorous behavioral repertoire to defend his territory and attract females (Fernald 1977; Fernald and Hirata 1977a,b). In contrast, when subordinate (SUB), males will shoal with conspecifics and females, display fewer and less conspicuous behavioral patterns, and adopt cryptic coloration that allows them to blend in with the surrounding environment (Fernald and Hirata 1977b). During social interactions, male cichlids produce sounds (Miguel Simões et al. 2008; Ripley et al. 2002) that females evaluate to assess the quality of potential mates (Verzijden et al. 2010). Based on the differences in coloration and behavior, DOMs are more vulnerable to predation than SUBs (Fernald and Hirata 1977a; Maan et al. 2008). On the other hand, executing startle-escapes is not only energetically costly, but also disruptive to ongoing behavioral activity, e.g., during foraging (Jones and Godin 2010; Krause and Godin 1996; Ydenberg and Dill 1986). Therefore, we ask whether startle responsiveness in this species differs between the two social phenotypes and whether these differences can be identified at the neural level.

Almost all animals show startle behavior—often, although not necessarily, followed by escape movements—in response to abrupt and unexpected stimuli of high intensity (Bennett 1984). In teleost fishes, the neural basis of startle-escape behavior has been studied in much detail (for recent reviews, see Eaton et al. 2001; Korn and Faber 2005). The behavior is controlled by the distinct synaptic, cellular, and network properties of identifiable reticulospinal neurons. The system is anchored by a pair of Mauthner neurons (M-cells) on which multimodal inputs converge (Canfield 2003; Eaton and Emberley 1991; Furukawa and Ishii 1967; Preuss et al. 2006; Szabo et al. 2006; Zottoli et al. 1987). A single action potential (AP) in one M-cell reliably activates contralateral spinal motor neurons causing a fast body-bend (C-start) away from a potential threat (Eaton et al. 1977; Preuss and Faber 2003; Weiss et al. 2006, 2009; Zottoli 1977). Startle probability is a quantifiable behavioral measure that reflects the excitability of the M-cell system remarkably well (Neumeister et al. 2008; Preuss and Faber 2003). Because of its unusual size and command-like role in the decision to execute a C-start (Kupferman and Weiss 1978), the M-cell–mediated startle-escape system offers

* H. Neumeister and K. W. Whitaker contributed equally to this work.
† H. A. Hofmann and T. Preuss contributed equally to this work.

Address for reprint requests and other correspondence: T. Preuss, Dept. of Psychology, Hunter College, City University of New York, 695 Park Ave., New York City, NY 10065 (E-mail: tpreuss@hunter.cuny.edu).

a unique opportunity to unravel the neural basis of status dependent plasticity.

In this study, we show that, in *A. burtoni*, startle responsiveness differs between the dominant and subordinate phenotypes and that this plasticity is mediated by status dependent differences in inhibitory drive and associated changes in M-cell input resistance.

METHODS

Animals

Adult *Astatotilapia* (formerly *Haplochromis*) *burtoni* from a laboratory-reared stock were housed in acrylic tanks (30 × 30 × 60 cm) in communities of 5–12 males and 5–12 females under conditions mimicking the natural environment in their native Lake Tanganyika (pH 8.5 ± 0.2; 27 ± 0.2°C; 12-h:12-h light:dark cycle). Gravel substrate and terracotta pots were provided to allow multiple males to establish territories within each community. For the individuals used in this study, we assessed dominance status twice weekly over a period of at least three weeks to identify stable DOMs and SUBs using established methods (Renn et al. 2008). All experimental protocols were performed in accordance with relevant guidelines and regulations of Hunter College of the City University of New York and The University of Texas at Austin.

Behavior

To assess the robustness of the hypothesized responses across experimenters and laboratories, we conducted the behavioral experiments at two different locations with just minor differences (*series 1* at Hunter College, NY, and *series 2* at The University of Texas at Austin). Specifically, these differences include slight variations in stimulation intensities, number of trials, and duration of intertrial intervals.

In *series 1* at Hunter College, we used a circular acrylic tank (76 cm diam, 20 cm water height) connected to a water reservoir with a heating unit for maintaining 27 ± 1°C water temperature. The tank was mounted onto an antivibration table to eliminate external mechanosensory cues. Surrounding opaque covers and a curtain eliminated external visual cues. Ventral views of the freely swimming fish were recorded via a mirror placed below the tank at a 45° angle, using a high-speed video camera (resolution 512 × 384 pixels; 1,000 frames/s; Kodak Extapro 1000 HRC, Eastman Kodak, San Diego, CA). The camera recorded a 28 × 21.5 cm area in the center of the tank at high magnification for detailed kinematic and latency analysis of the behavior. Video recordings of responses were stored on a DV tape or DVD.

Sound stimuli were produced by one of two underwater loudspeakers (UW-30, University Sound, Buchanan, MI) positioned on opposite sites of the experimental tank supported within a 6 cm thick layer of foam lining the entire inner wall. The sequence of speaker activation was random. The stimulus was a sound pip created as a 200 Hz single sine wave in Igor Pro (WaveMetrics, Portland, OR) with five distinct intensities ranging from 130 to 170 dB in water with a reference (re.) pressure of 1 μPa (note: airborne sounds are typically reported with respect to a reference pressure level of 20 μPa, which translates to a stimulus range of ~68–108 dB SPL). A typical experiment consisted of 20 trials. To test fish in a similar state of activity, experiments continued only when they resumed swimming after stimulation; thus intertrial intervals varied from 1 to 58, with a mean of 8.3 ± 2.5 (SD) min for DOMs and a mean of 7.52 ± 1.56 min for SUBs.

Stimulus onset was marked on the high-speed video image by a light-emitting diode mounted in the optical path outside of the tank; the fish did not see this marker. In addition, the waveform and amplitude of the auditory stimuli were recorded using SQ01 hydrophones (Sensor Technology, Collingwood, Ontario, Canada) located at the tank wall near and between the loudspeakers.

In *series 2* at The University of Texas at Austin, we used a rectangular 110 liter acrylic tank with two underwater speakers (UW-30, Electro Voice, Burnsville, MN) on opposite ends. A black curtain around the tank eliminated visual cues. Six lights, 55 W fluorescent lamps (B&H Photo), mounted above the tank provided illumination for the high-speed camera (same as specified above in *series 1*) during filming against an opaque bottom; this is more naturalistic, yet results in reduced contrast and thus decreased accuracy when determining the precise onset of the startle behavior. Permanent records of startle responses were recorded digitally with a KWorld Xpert DVD Maker USB 2.0 Video Capture Device (KWorld, Irvine, CA). A 200 Hz sine wave pulse was created by a waveform generator (Wavetek) and sent through an amplifier (AudioSource). The amplifier allowed the experimenter to choose a speaker and control the sound intensity on each trial. Each fish was presented with three blocks of four different stimulus intensities (in randomized order), ranging from 140 to 175 dB re. 1 μPa in water, with variable intervals between trials ranging from 2 to 10 min. In both experimental series, we transferred individual test animals from their home tanks into a central circular arena (30 cm diam, 20 cm high) inside the experimental tank. Acclimation time before the presentation of sound stimuli was 30–60 min, and an experiment typically lasted 2–4 h.

Probability and latency of sound-evoked responses were analyzed as described previously (Preuss and Faber 2003). Individual startle probabilities were calculated from the number of C-starts occurring within a given number of trials. Response latency, defined as the first detectable movement of the head after stimulus onset, was determined from successive video frames with a time resolution of 1 ms. We note that in both experimental series, high-speed video was used to distinguish M-cell initiated escapes to abrupt auditory stimuli (with a characteristic latency of 9–12 ms) from potential non–M-cell–initiated responses (Zottoli et al. 1999). However, in *series 1,* we used a narrower range of stimulus intensities compared with the data set of *series 2*. Therefore the stimulus response curve was made for *series 2* data only. On the other hand, in *series 2,* optical limitation allowed for a slightly less accurate determination of movement onset and added ~1 ms ambiguity for latency measurements compared with *series 1*. Thus we used only data from *series 1* for the latency comparison.

Electrophysiology

These experiments involved standard in vivo surgical and recording techniques used previously (Preuss and Faber 2003). Fish were initially anesthetized by immersion in MS-222 (120 mg/l). A topical anesthetic (20% benzocaine gel, Ultradent) was applied at the incision site on the body and the dorsal cranium for 5 min before dissection. The fish was stabilized in the recording chamber by two pins, one on each side of the head, further immobilized with intramuscular injections of D-tubocurarine (1–3 μg/g body weight), and respirated through the mouth with a steady flow of aerated saline containing the general anesthetic MS-222 at a concentration of 20 mg/l. This concentration has been shown to have little if any effect on the spontaneous activity and mechanosensory responses of peripheral sensory nerves in fish (Palmer and Mensinger 2004). The recording chamber was mounted inside an opaque, thin-walled chamber filled with temperature-controlled (27°C) saline covering the fish up to just above its eyes. A small hole was made in the cranium to expose the medulla for somatic M-cell recordings. A small lateral incision at the caudal mid-body was made for exposure of the spinal cord. Bipolar electrodes were placed on the unopened spinal cord for antidromic activation of the M-axons with small pulses (5–8 V) using an isolated stimulator. Antidromic stimulation produces a negative potential in the M-cell axon cap (typically >15 mV), which unambiguously identifies its axon hillock and allows intracellular recordings from the

M-cell soma or along the lateral dendrite at defined distances from the axon hillock (Faber and Korn 1978; Furukawa 1966).

Postsynaptic responses (PSPs) to sound stimuli and action potentials in response to antidromic stimulation were recorded in the M-cell with sharp glass electrodes (10–12 MΩ) filled with 5 M potassium acetate using an Axoprobe-1A amplifier in current-clamp mode. Sound stimuli consisted of 200 Hz sound pips produced by a subwoofer with underwater intensities ranging from 126 to 133 dB re. 1 μPa in water. Auditory stimuli were recorded with a microphone positioned above the fish during the experiments and with a hydrophone (SQ01, Sensor Technology) inside the recoding chamber tank for stimulus calibration trials. Stimulus traces were stored on-line together with the intracellular recordings using a Macintosh G5 equipped with a data acquisition card (National Instruments, Austin, TX) and acquisition software developed in the laboratory (sampling rate, 30–50 kHz). Throughout the experiments (typically 2–3 h), we monitored the M-cell resting membrane potential (RMP) as a measure for the quality of the recording and the sustained health of the M-cells. Cells with an RMP less negative than −76 mV and experiments with >10% changes in RMP were excluded.

Although the recordings were made in submerged fish to resemble the behavioral stimulus conditions, potential experimental confounds have to be considered that may influence the underwater sound stimulus in the physiology setup. First, the fixation of the animals for the recordings distorts the particle displacement component of underwater sounds. Second, underwater speakers could not be used in the physiology experiments because of electric noise interference. Instead we used a shielded subwoofer in close distance to the physiology setup to create sound pips. Hydrophone recordings showed that this reduced the achievable maximal underwater sound intensity by ~20 dB (re. 1 μPa) compared with the behavioral experiments.

Data analysis and statistics

Unless otherwise noted, data are reported as mean ± SE and were analyzed using a single-factor ANOVA and nonparametric tests as indicated in the text. For the behavioral data obtained in *series 1*, we performed a χ^2 analysis. When we replicated these results in *series 2* with a modified testing protocol, with each fish undergoing fewer trials, we applied a more conservative statistical bootstrap analysis of the sampling distributions. Significance levels were set at $P = 0.05$. Sigmoid curve fits for the stimulus–response curves were generated in IGOR PRO (Wavemetrics), using the following function, *base* + *max*/{1 + exp[(*xhalf* − *x*)/*rate*]},where the coefficient *base* sets the *y* value at small *x*; *base* +*max* sets the *y* value at large *x*; *xhalf* sets the *x* value at which *y* is at (*base* + *max*)/2; and *rate* sets the rise rate. Finally, measurements of the synaptic responses and the inhibitory shunt recorded in the M-cell were made in averaged traces ($n = 5$) using custom software and IGOR PRO.

RESULTS

Behavior

A. burtoni males responded to an abrupt auditory click with a powerful short latency startle escape (C-start). As described previously for goldfish, these responses include two kinematic stages: a short-latency, powerful body bend forming a C-shape (stage 1) followed by a return flip associated with forward propulsion (stage 2; Eaton et al. 1977; Foreman and Eaton 1993).

In the first series of experiments, we compared startle responsiveness of the two phenotypes and found a significantly higher ($\chi^2 = 6.34$, df = 1, $P = 0.025$, sample size = 439) probability in DOMs (55.9 ± 3.9%, $n = 11$) compared with SUBs (44.3 ± 5.0%, $n = 11$; Fig. 1*A*). We replicated this finding in *series 2* (DOMs 58.3 ± 2.9%, $n = 14$; SUBs 41.7 ± 2.0%, $n = 18$; Fig. 1*B*). Bootstrap analysis of the sampling distributions showed no overlap at $P = 0.01$. To compare behavioral threshold in both morphs, we constructed a stimulus–response curve with data from *series 2* that were fitted with a sigmoid function (Fig. 1*C*). The results show, for DOMs, a shift of the stimulus–response curve to the lower stimulus intensities compared with SUBs, which indicates an overall higher responsiveness for all but the highest stimulus intensities. The extrapolated behavioral threshold, defined as the stimulus intensity evoking an escape probability of 0.5, was 154.61 ± 1.23 dB for DOMs and 158.29 ± 1.38 dB in SUBs (Fig. 1*C*, dashed lines).

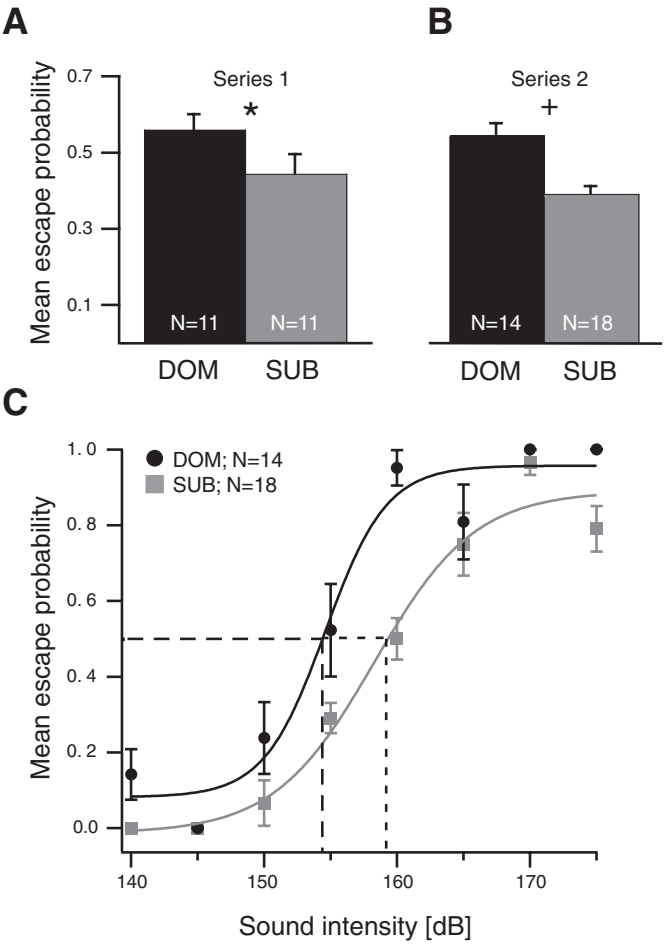

FIG. 1. Influence of social rank on startle-escape behavior. *A* and *B*: mean escape probabilities (±SE) in dominants (DOMs) and subordinates (SUBs) for auditory stimulus *paradigms 1* (*A*) and *2* (*B*). Note: these results involved fish populations used for experiments in different laboratories, underlining the reproducibility of the results. *Series 1*: *P = <0.025; *series 2*: +$P < 0.01$. *C*: stimulus–response curves for DOMs (black) and SUBs (gray) from the data in *B* (means ± SE). Narrow and wide-gaped dashed lines indicate the stimulus intensity that evokes a response 50% of the time, showing the greater sensitivity of DOMs. Sigmoid fit coefficients ± SD for DOMs (base = 0.08 ± 0.08; max = 0.87 ± 0.11; xhalf = 154.61 ± 1.23; rate = 2.3037 ± 1.2) and SUBs (base −0.013 ± 0.06; max = 0.90 ± 0.11; xhalf = 158.29 ± 1.38; rate = 3.7739 ± 1.32). Note: smaller rate indicates a faster rise.

In *series 1*, latencies between stimulus onset and initiation of C-start behavior (stage 1) did not significantly differ between DOMs and SUBs, averaging 11.4 ± 0.3 and 11.9 ± 0.3 ms, respectively (*t*-test, $P = 0.29$). Latencies could not be measured as accurately in *series 2*, but fell also into the 11–12 ms

range for both DOMs and SUBs. These values are characteristic of the latencies measured in the M-cell–mediated auditory-induced startle behavior (Preuss and Faber 2003).

Electrophysiology

Because of its central role in triggering startle escape behavior in teleosts, we hypothesized that the M-cell system is the locus of the observed plasticity (Preuss and Faber 2003; Weiss et al. 2006; Zottoli 1977). Accordingly, we compared the amplitude and waveform of sound-evoked PSPs recorded in the M-cell soma in response to sound pips (200 Hz) in DOMs ($n = 7$) and SUBs ($n = 5$). Figure 2*A* shows averaged traces (5 sweeps) from a DOM (black) and SUB (gray) in response to a 133 dB re. 1μPa sound pip. In both morphs, the evoked PSPs showed an initial steep component followed by a complex, long-lasting membrane depolarization. The latter was characterized by successive transient PSP peaks that are superimposed onto an underlying slowly decaying depolarization. Similar composite PSPs can be distinguished in M-cells of goldfish, where they reflect fast electrotonic coupling potentials and long-lasting glutamatergic synaptic currents, which are mediated by the mixed eighth nerve synapses that impinge onto the M-cell lateral dendrite (i.e., the fast and slow PSPs in Szabo et al. 2006). PSP mean onset times varied from 3.2 to 1.8 ms and decreased with increasing sound intensities; however, PSP onsets did not significantly differ between DOMs and SUBs (Fig. 2*B*). The peak amplitude of the compound PSP typically occurred 4–6 ms after onset (Fig. 2*A*) and also varied with stimulus intensity (range: 126–133 dB) from 2.9 to 8.7 and 1.8 to 7.6 mV in DOMs and SUBs, respectively. Indeed, for the two highest stimulus intensities, the mean PSP peak amplitudes in DOMs were significantly larger compared with SUBs (126 dB, $F_{1,11} = 2.61$, $P = 0.137$; 130 dB, $F_{1,12} = 6.56$, $P = 0.026$; 133 dB, $F_{1,11} = 7.96$, $P = 0.018$; Fig. 2*C*). In addition, we found that in four of six DOMs, higher-intensity sounds evoked M-cell APs in 5–8% of the trials. In contrast, the same stimuli evoked only subthreshold responses in SUBs ($n = 5$).

No significant differences were found for the M-cell RMP (RMP means: DOMs −79 ± 1.6 mV; SUBs −81.2 ± 1.1 mV; $F_{1,11} = 1.07$; $P = 0.323$) or for the amplitude of antidromically evoked somatic APs (means: DOMs 41.15 ± 5.2 mV; SUBs 35.6 ± 3.3 mV; $F_{1,11} = 0.63$; $P = 0.442$). The relatively negative RMP and low AP amplitude values are typical for M-cells and indicate their high firing threshold and low input resistance (Faber and Korn 1978; Faber et al. 1991).

Taken together, the physiological results show differences in the M-cell synaptic response to sound stimuli that complement our behavioral results, i.e., the higher behavioral responsiveness of DOMs. The relatively low occurrence of APs in DOMs and their absence in SUBs compared with the observed behavioral response rate is likely caused by the lower maximal intensity of underwater stimuli used in the physiology setup because of technical constraints (see METHODS).

One possible mechanism for the differences in the synaptic response would be a status-dependent change of M-cell excitability. This notion is based on the fact that well-delineated feedback and feedforward inhibitory networks control M-cell excitability and startle escape threshold via classical chemical (glycinergic), but also electrical field (ephaptic) inhibition (Faber et al. 1991; Furukawa and Furshpan 1963; Preuss and Faber 2003; Preuss et al. 2006; Weiss et al. 2008). Chemical inhibition is mediated by a Cl^--dependent change in membrane conductance that effectively decreases the M-cell input resistance (Faber and Korn 1982). Because the M-cell RMP is close to the Cl^- equilibrium potential, inhibition does not produce any measurable hyperpolarization. However, the relative change in input resistance produced by this inhibition can be quantified as the fractional reduction in peak amplitude (inhibitory shunt) of an evoked test AP after activating either the feedback (Fig. 3*A1*) or the feedforward (Fig. 3*B1*) inhibitory network with an appropriate conditioning stimulus (Faber and Korn 1978). This approach is possible because the M-cell's soma and dendrites are unexcitable (Furshpan and Furukawa 1962); thus an increase in the fractional shunt (defined as $100 - AP_{test}/AP_{control} \times 100$) indicates a decrease in input resistance (Faber and Korn 1982).

The feedback network can be activated by applying an antidromically evoked M-axon AP (conditioning AP in Fig. 3*A1*). Systematically changing the interstimulus interval (ISI) between the conditioning AP and the test AP exposes the

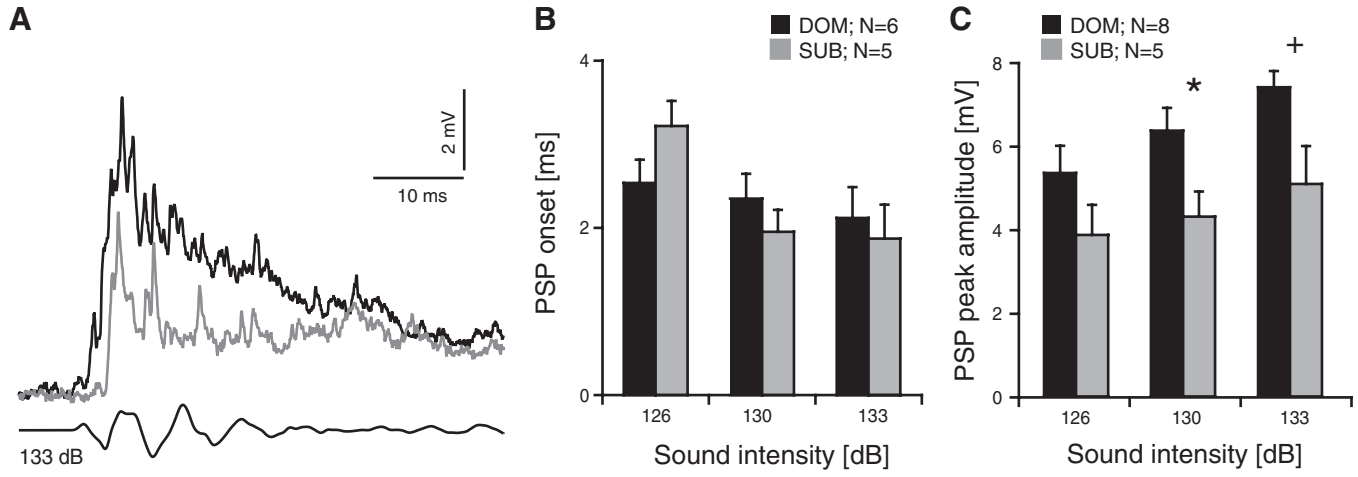

FIG. 2. Differential Mauthner cell (M-cell) responses in DOMs and SUBs. *A*: somatically recorded postsynaptic potentials (PSPs; (averages of 5 sweeps each) in a DOM (black) and a SUB (gray) in response to a 133 dB sound pip. Bottom trace: microphone recording of the sound stimulus. *B*: plots of PSP onset times (means ± SE) for 3 sound intensities. *C*: plots of mean PSP peak amplitudes (±SE) for 3 sound intensities. *$P = 0.026$; +$P = 0.018$.

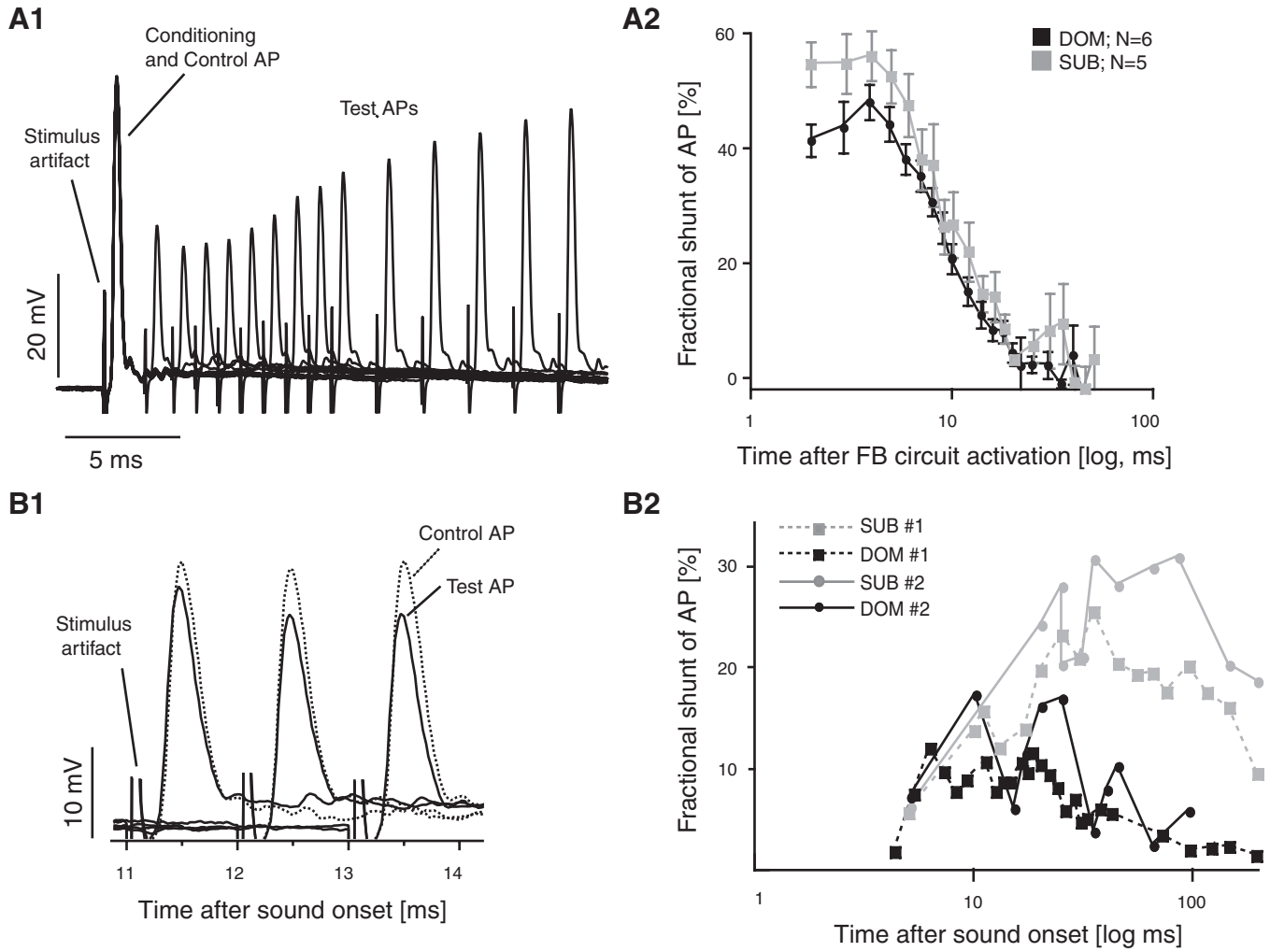

FIG. 3. Socially controlled inhibitory drive in the M-cell. Feedback inhibition. *A1*: somatically recorded test action potentials (APs) in a DOM after an evoked AP as conditioning stimulus. *A2*: magnitude of the inhibitory shunt plotted against the interstimulus interval (ISI) between conditioning and test AP in DOMs and SUBs (means ± SE; $n = 5$). Feedforward inhibition. *B1*: somatically recorded M-cell APs in a SUB at different ISIs with (solid lines) and without (dashed lines) a preceding sound click of 130 dB (M-cell sound response not shown). *B2*: magnitude of the inhibitory shunt for 2 DOMs (black) and 2 SUBs (gray) plotted against ISI.

evoked inhibitory time course. Figure 3*A2* shows the mean fractional shunt over a range of ISIs (2–20 ms) for DOMs ($n = 6$) and SUBs ($n = 5$). Overall, both morphs show a comparable inhibitory time course, namely a powerful initial component and a rapid decay to baseline within 20 ms. However, at onset and for ~4 ms thereafter, inhibition was more pronounced in SUBs, as indicated by a significant difference in peak shunt amplitude (SUBs: 59.3 ± 3.6%; DOMs: 46.3 ± 3.2%; *t*-test, $t = -2.69$, df = 8, $P = 0.026$). Later parts (>9 ms) of the inhibitory time course overlap.

Feedforward inhibition is provided by a population of interneurons that receive electrotonic and chemical input from eighth nerve afferences and can be activated by sound stimuli. Again, this inhibition can be quantified by the fractional reduction of a test AP at distinct ISIs after the sound stimulus (Fig. 3*B1*). Figure 3*B2* shows the individual inhibitory time courses for two DOMs and two SUBs in response to a 130 dB sound pip. In all cases, inhibition starts gradually after sound onset; however, the individual time courses were highly variable and long-lasting, which likely reflects the graded rather than synchronic activity of the inhibitory interneurons. Accordingly, we quantified these complex waveforms by means of their RMS value over the initial 50 ms for six DOMs and five SUBs and found significantly higher mean values for the fractional inhibitory shunt in SUBs (15.56 ± 2.9%) compared with DOMs (8.48 ± 5.3%; *t*-test: $t = -2.61$, df = 6, $P = 0.037$).

DISCUSSION

In this study, we used two different experimental data sets (*series 1* and *2*) to show that startle responsiveness of male *A. burtoni* depends on their positions in a social hierarchy. The startle behavior is governed by a medullar circuit centered on a pair of decision-making neurons (M-cells), which integrate massive excitatory and inhibitory inputs. M-cells have a high firing threshold, and the generation of an AP in one of the neurons determines the likelihood, timing, and direction of the behavior (Eaton and Emberley 1991; Preuss et al. 2006; Weiss et al. 2006, 2009). In addition, M-cell excitability can be modified by experience and environmental conditions (Oda et al. 1998; Preuss and Faber 2003; Szabo et al. 2008), and M-cell

activity is also associated with voluntary behavior (Canfield and Rose 1996; Schlegel and Schuster 2008). Thus this system presents a superb opportunity to study the neurobiological mechanisms of adaptive plasticity and decision-making in its natural context at several levels of biological organization.

We found that latencies of startle escapes did not differ between social phenotypes. The observed short latencies are typical for M-cell–mediated auditory startles, reflecting the direct, disynaptic afferent pathway described for various teleost species (Eaton et al. 1977; Fetcho and Faber 1988; Furukawa and Ishii 1967; Preuss and Faber 2003; Weiss et al. 2006, 2008; Zottoli 1977). The cited studies established with intracellular and chronic recordings a 1.5 ms synaptic delay in the auditory afferents, a 2–4 ms processing time in the M-cell, and a minimum interval of 6–8 ms between the generation of the M-cell AP and the onset of movement. In other words, acoustically evoked C-starts involving the M-cell are characterized by latencies that approach a physiological minimum delay, and ablation of the M-cells significantly increases the mean startle latency (Lui and Fetcho 1999; Zottoli et al. 1999). In principle, DOMs and SUBs could use different motor pathways with distinct latencies, e.g., one that involves reticulospinal neurons, other than the M-cell (Kohashi and Oda 2008; Ritter et al. 2001), similar to the scenario found for giant axon and nongiant motor pathways of the socially regulated escape response in crayfish (Edwards et al. 1999; Yeh et al. 1996). Thus the fact that latencies are similarly short in both morphs strongly implies that the startle responses to auditory stimuli are produced by the same sensorimotor pathway, namely the M-cell startle circuit.

Although latencies did not differ, we observed a higher behavioral responsiveness and a lower stimulus threshold in DOMs. These observations were complemented by our electrophysiological results that show a higher excitability of M-cells in DOMs. Decreasing stimulus threshold effectively increases the critical distance at which to respond to an approaching predator (Dill 1990; Godin and Dugatkin 1996; Martin and Lopez 1999; Ydenberg and Dill 1986). Thus the observed startle plasticity in DOMs and SUBs can be understood as an adaptation to differences in predation pressure. At this point, we can only speculate on the driving force underlying this adaption. However, as noted above, two candidates are the more conspicuous: coloration and the fighting behavior of DOMs, which likely attract the attention of predators (Maan et al. 2008). In fact, DOMs engaged in fights show delayed escape onsets when confronted with an approaching visual threat in the Golden Dwarf Cichlid, *Nannacara anomala,* (Brick 1998), and in *A. burtoni* (Hofmann, unpublished observations), likely because of their attention being diverted by social interactions. It is important to note that such gradually building visual stimuli (looms) evoke M-cell startles with much longer and variable latencies compared with those evoked by abrupt sounds (Canfield 2003; Preuss et al. 2006; Weiss et al. 2006), which likely reflects the added processing steps in the polysynaptic visual pathway (Preuss et al. 2006; Zottoli et al. 1987).

Interestingly, *A. burtoni* females can become phenotypically dominant in a social environment lacking males without changing sex (S.C.P. Renn and H. A. Hofmann, unpublished data), which allows us to ask whether conspicuous coloration in these females is also tied to an adaptive change in escape responsiveness.

Our electrophysiological results suggest that startle plasticity in DOMs and SUBs is produced by a socially regulated shift in M-cell excitability, indicated by the differential PSP peak amplitudes and different levels of evoked feedforward and feedback shunting inhibition. As noted, feedforward inhibition is mediated by a population of interneurons (PHP cells) presynaptic to the M-cells that receive electrotonic and chemical synaptic input from auditory afferents (Faber et al. 1991; Preuss and Faber 2003; Weiss et al. 2008). This mostly dendritic inhibition is powerful because it effectively shunts incoming excitatory synaptic currents out from the cell through glycine and GABA-gated Cl^- channels (Faber and Korn 1988). Indeed, shunting inhibition is considered to have a divisive effect on subthreshold membrane depolarizations (rather than the subtractive effect of hyperpolarization) and thus provides a potent modulatory mechanism for gain control

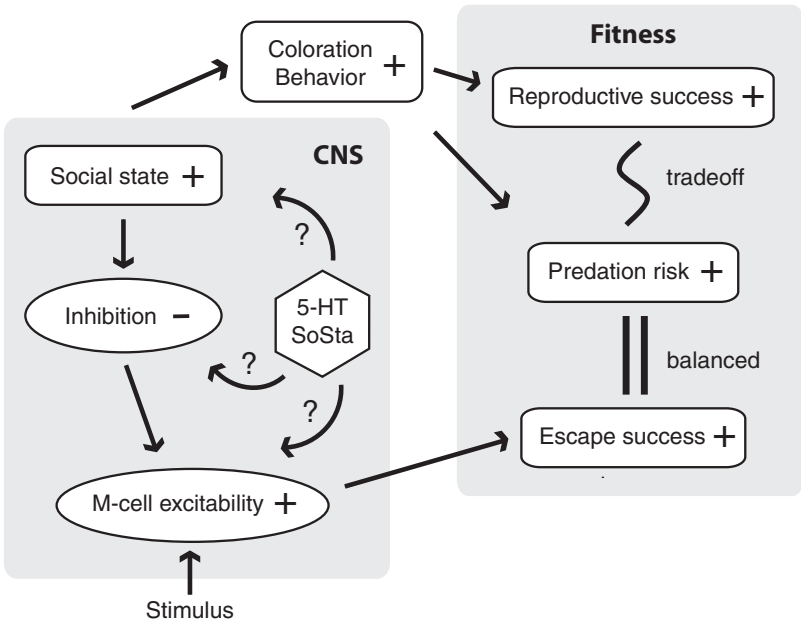

FIG. 4. A model summarizing the social regulation of startle-escape responsiveness in *A. burtoni*, acting through the M-cell system and creating a fitness-relevant trade-off (denoted by ~) between reproductive success and predation risk (which is balanced by escape success, indicated by =). The depicted scenario is for DOMs and the signs would reverse for SUBs. Serotonin (5-HT) and somatostatin (SoSta) are promising candidates (indicated by question marks) for mediating this plasticity at the level of the CNS.

(Prescott and De Koninck 2003). Thus the less potent feedforward inhibition observed in DOMs will result in a relatively higher M-cell excitability immediately after a stimulus.

A comparable dendritic feedforward inhibitory circuit has been described in the crayfish startle escape system where it provides for a temporal filter that allows only abrupt stimuli to activate the lateral giant neuron (Vu et al. 1997). Activation of the M-cell appears less restrictive because both abrupt acoustic and gradually building visual looms evoke M-cell–mediated startles (Preuss et al. 2006; Weiss et al. 2006). The scenario of a diving bird breaking the water surface provides an ecological context for such stimuli. Against this background, it is interesting to note that visual and acustico-lateralis inputs impinge onto separate dendrites, with potentially different temporal processing properties (Preuss, unpublished results).

As in the feedforward inhibitory system, we also observed state-dependent differences in the feedback inhibitory network (Fig. 3*B*), which are consistent with a more excitable M-cell in DOMs. This difference between the morphs can be explained by a shift of the input–output characteristics in the inhibitory interneurons that provide strong collateral inhibition in the M-cell soma. These interneurons are synchronously excited by a single M-cell axon AP, which prevents repetitive firing of the M-cells (Furukawa and Furshpan 1963); however, these neurons also receive afferent inputs (Faber and Korn 1978). Overall, these results imply a lower inhibitory tone in the M-cells of DOMs that can explain the increased synaptic responses (PSPs), the higher behavioral responsiveness, and the behavioral shift observed in the stimulus–response curves in this morph (Fig. 1*C*).

Such changes in inhibitory tone can be explained by status-dependent changes in excitability of the inhibitory neurons themselves and/or by alterations in the efficacy of the inhibitory connection impinging onto the M-cell membrane mediated by pre- and/or postsynaptic mechanism (i.e., changes in transmitter release or postsynaptic receptor density). However, our experiments cannot exclude the possibility that the larger PSPs in DOMs may be also mediated by modulating the efficacy of excitatory synaptic transmission at the mixed electrotonic and chemical junctions between the large eighth nerve endings and the M-cell (Pereda et al. 1992, 1994). For example, in goldfish, local application of the neuropeptide somatostatin onto the M-cell lateral dendrite increases excitatory synaptic transmission (Pereda et al. 1997), and somatostatin has been shown to be co-localized with glutamatergic excitatory but also with GABAergic inhibitory synaptic contacts onto the M-cell (Sur et al. 1994). These findings are interesting because somatostatin also controls social behavior in *A. burtoni* (Hofmann and Fernald 2000; Trainor and Hofmann 2006, 2007) and thus constitutes one candidate for the proposed neuromodulatory link between social state and M-cell excitability. Social control of escape behavior and modification of the underlying neural circuitry (such as the lateral giant neuron system) have been extensively studied in crayfish, emphasizing the pivotal role of serotonin in these processes (Antonsen and Edwards 2007; Edwards and Kravitz 1997; Edwards et al. 1999, 2003; Spitzer et al. 2005; Yeh et al. 1996, 1997). It is thus interesting to note that local injection of 5-HT enhances tonic and evoked inhibitory currents in the M-cell (Mintz and Korn 1991; Mintz et al. 1989). Moreover, subordinate cichlids show higher levels of 5-HT and 5-HT metabolite ratios in the brain stem and telencephalon compared with their dominant counterparts (Winberg et al. 1997), and intracranially injected 5-HT inhibits aggressive responsiveness in these fish (Munro 1986). Thus 5-HT is another possible candidate for a neuromodulatory link between social state and the M-cell excitability system.

Based on these considerations, we propose a model for how the life history trade-off between social and ecological factors experienced by male *A. burtoni* is implemented at the level of the simple circuitry that is centered on the M-cells (Fig. 4). DOM status is defined by striking color patterns and vigorous behavioral activity, which are essential to reproductive success. However, these conspicuous traits result in increased predation risk compared with SUBs. To accommodate this trade-off at the level of the nervous system, reduction in the inhibitory drive onto the M-cell leads to an increased M-cell excitability in DOMs, possibly mediated by 5-HT and/or somatostatin. As a consequence, even under constant stimulus conditions, DOMs show an increased startle responsiveness that facilitates successful predator avoidance. Taken together, this model provides a number of testable hypotheses regarding the role of neuromodulators in mediating the fitness trade-off between reproduction and ecology. It also allows us to make predictions about M-cell plasticity across populations that might differ in predation pressure and/or conspicuousness of reproductive males.

ACKNOWLEDGMENTS

We thank members of the Hofmann and Preuss laboratories for discussion and P. Dijkstra, M. Markham, and V. Medan for critically reading earlier versions of this manuscript.

GRANTS

This work was supported by National Science Foundation Grants 0946637 to T. Preuss and 0751311 to H. A. Hofmann, Hunter College, City University of New York to T. Preuss, Research Foundation of City University of New York to T. Preuss, the Alfred P. Sloan Foundation, the Institute for Cellular and Molecular Biology at The University of Texas at Austin to H. A. Hofmann, and the Department of Defense Science, Mathematics and Research for Transformation program to K. W. Whitaker.

DISCLOSURES

No conflicts of interest, financial or otherwise, are declared by the authors.

REFERENCES

Antonsen BL, Edwards DH. Mechanisms of serotonergic facilitation of a command neuron. *J Neurophysiol* 98: 3494–3504, 2007.

Bennett MVL. Escapism: some startling revelations. In: *Neural Mechanisms of Startle Behavior*, edited by Eaton RC. New York: Plenum Press, 1984, p. 353–362.

Brick O. Fighting behaviour, vigilance and predation risk in the cichlid fish *Nannacara anomala*. *Anim Behav* 56: 309–317, 1998.

Canfield JG. Temporal constraints on visually directed C-start responses: behavioral and physiological correlates. *Brain Behav Evol* 61: 148–158, 2003.

Canfield JG, Rose GJ. Hierarchical sensory guidance of Mauthner-mediated escape responses in goldfish *Carassius auratus* and cichlids *Haplochromis burtoni*. *Brain Behav Evol* 48: 137–156, 1996.

Dijkstra PD, Hekman R, Schulz RW, Groothuis TGG. Social stimulation, nuptial colouration, androgens and immunocompetence in a sexual dimorphic cichlid fish. *Behav Ecol Sociobiol* 61: 599–609, 2007.

Dill LM. Distance-to-cover and the escape decisions of an African cichlid fish, *Melanochromis chipokae*. *Environ Biol Fish* 27: 147–152, 1990.

Eaton RC, Bombardieri RA, Meyer DL. The Mauthner-initiated startle response in teleost fish. *J Exp Biol* 66: 65–81, 1977.

Eaton RC, Emberley DS. How stimulus direction determines the trajectory of the Mauthner-initiated escape response in a teleost fish. *J Exp Biol* 161: 469–487, 1991.

Eaton RC, Lee RK, Foreman MB. The Mauthner cell and other identified neurons of the brainstem escape network of fish. *Prog Neurobiol* 63: 467–485, 2001.

Edwards DH, Heitler WJ, Krasne FB. Fifty years of a command neuron: the neurobiology of escape behavior in the crayfish. *Trends Neurosci* 22: 153–161, 1999.

Edwards DH, Issa FA, Herberholz J. The neural basis of dominance hierarchy formation in crayfish. *Microsc Res Tech* 60: 369–376, 2003.

Edwards DH, Kravitz EA. Serotonin, social status and aggression. *Curr Opin Neurobiol* 7: 812–819, 1997.

Endler JA. Predation, light intensity and courtship behaviour in *Poecilia reticulata*. *Anim Behav* 35: 1376–1385, 1978.

Endler JA. Variation in the appearance of guppy color patterns to guppies and their predators under different visual conditions. *Vision Res* 31: 587–608, 1991.

Faber DS, Korn H. *Neurobiology of the Mauthner Cell.* New York: Raven Press, 1978.

Faber DS, Korn H. Transmission at a central inhibitory synapse. I. Magnitude of unitary postsynaptic conductance change and kinetics of channel activation. *J Neurophysiol* 48: 654–678, 1982.

Faber DS, Korn H. Unitary conductance changes at teleost Mauthner cell glycinergic synapses: a voltage-clamp and pharmacologic analysis. *J Neurophysiol* 60: 1982–1999, 1988.

Faber DS, Korn H. Applicability of the coefficient of variation method for analyzing synaptic plasticity. *Biophys J* 60: 1288–1294, 1991.

Faber DS, Korn H, Lin JW. Role of medullary networks and postsynaptic membrane properties in regulating Mauthner cell responsiveness to sensory excitation. *Brain Behav Evol* 37: 286–297, 1991.

Fernald RD. Quantitative behavioral observations of *Haplochromis burtoni* under semi-natural conditions. *Anim Behav* 25: 643–653, 1977.

Fernald RD. Social regulation of the brain: sex, size and status. *Novartis Found Symp* 244: 169–184, 2002.

Fernald RD, Hirata NR. Field studies of *Haplochromis burtoni*: quantitative behavioral observations. *Anim Behav* 25: 964–975, 1977a.

Fernald RD, Hirata NR. Field study of *Haplochromis burtoni*: habitats and co-habitants. *Environ Biol Fish* 2: 299–308, 1977b.

Fetcho JR, Faber DS. Identification of motoneurons and interneurons in the spinal network for escapes initiated by the Mauthner cell in goldfish. *J Neurosci* 8: 4192–4213, 1988.

Foreman MB, Eaton RC. The direction change concept for reticulospinal control of goldfish escape. *J Neurosci* 13: 4101–4113, 1993.

Furshpan EJ, Furukawa T. Intracellular and extracellular responses of the several regions of the Mauthner cell of the goldfish. *J Neurophysiol* 25: 732–771, 1962.

Furukawa T. Synaptic interaction at the Mauthner-cell of goldfish. *Prog Brain Res* 21: 44–70, 1966.

Furukawa T, Furshpan EJ. Two inhibitory mechanisms in the Mauthner neurons of goldfish. *J Neurophysiol* 26: 140–176, 1963.

Furukawa T, Ishii Y. Neurophysiological studies on hearing in goldfish. *J Neurophysiol* 30: 1377–1403, 1967.

Gilmour KM, Wilson RW, Sloman KA. The integration of behaviour into comparative physiology. *Physiol Biochem Zool* 78: 669–678, 2005.

Godin JG, Dugatkin LA. Female mating preference for bold males in the guppy, *Poecilia reticulata*. *Proc Natl Acad Sci USA* 93: 10262–10267, 1996.

Godin JGJ, McDonough HE. Predator preference for brightly colored males in the guppy: a viability cost for a sexually selected trait. *Behav Ecol* 14: 194–200, 2003.

Hofmann HA. Functional genomics of neural and behavioral plasticity. *J Neurobiol* 54: 272–282, 2003.

Hofmann HA, Fernald RD. Social status controls somatostatin neuron size and growth. *J Neurosci* 20: 4740–4744, 2000.

Huhta E, Rytkonen S, Solonen T. Plumage brightness of prey increases predation risk: an among-species comparison. *Ecology* 84: 1793–1799, 2003.

Jones KA, Godin JJ. Are fast explorers slow reactors? Linking personality type and anti-predator behavior. *Proc R Soc Lond B Biol Sci* 277: 625–632, 2010.

Kohashi T, Oda Y. Initiation of Mauthner- or non-Mauthner-mediated fast escape evoked by different modes of sensory input. *J Neurosci* 28: 10641–10653, 2008.

Korn H, Faber DS. The Mauthner cell half a century later: a neurobiological model for decision-making? *Neuron* 47: 13–28, 2005.

Krause J, Godin JGJ. Influence of prey foraging posture on flight behavior and predation risk: predators take advantage of unwary prey. *Behav Ecol* 7: 264–271, 1996.

Kupferman I, Weiss KR. The command neuron concept. *Behav Brain Sci* 1: 3–39, 1978.

Liu KS, Fetcho JR. Laser ablations reveal functional relationships of segmental hindbrain neurons in zebrafish. *Neuron* 23: 325–335, 1999.

Lyytinen A, Brakefield PM, Mappes J. Significance of butterfly eyespots as an anti-predator device in ground-based and aerial attacks. *Oikos* 100: 373–379, 2003.

Maan ME, Eshuis B, Haesler MP, Schneider MV, van Alphen JJM, Seehausen O. Color polymorphism and predation in a Lake Victoria cichlid fish. *Copeia* 3: 621–629, 2008.

Martin J, Lopez P. An experimental test of the costs of antipredatory refuge use in the wall lizard, Podarcis muralis. *Oikos* 84: 499–505, 1999.

Miguel Simões J, Duarte IS, Fonseca PJ, Turner GF, Amorim MC. Courtship and agonistic sounds by the cichlid fish *Pseudotropheus zebra*. *J Acoust Soc Am* 124: 1332–1338, 2008.

Mintz I, Gotow T, Triller A, Korn H. Effect of serotonergic afferents on quantal release at central inhibitory synapses. *Science* 245: 190–200, 1989.

Mintz I, Korn H. Serotonergic facilitation of quantal release at central inhibitory synapses. *J Neurosci* 11: 3359–3370, 1991.

Munro AD. Effects of melatonin, serotonin, and naloxone on aggression in isolated cichlid fish, *Aequidens pulcher*. *J Pineal Res* 3: 257–262, 1986.

Neumeister H, Szabo TM, Preuss T. Behavioral and physiological characterization of sensorimotor gating in the goldfish startle response. *J Neurophysiol* 99: 1493–1502, 2008.

Oda Y, Kawasaki K, Morita M, Korn H, Matsui H. Inhibitory long-term potentiation underlies auditory conditioning of goldfish escape behaviour. *Nature* 394: 182–185, 1998.

Palmer LM, Mensinger AF. Effect of the anesthetic tricaine (MS-222) on nerve activity in the anterior lateral line of the oyster toadfish, *Opsanus tau.* *J Neurophysiol* 92: 1034–1041, 2004.

Pereda A, Reisine T, Faber DS, Korn H. Somatostatin enhances excitatory synaptic transmission at mixed synapses on the Mauthner (M-) cell. *Neurosci Soc Abstr* 23: 1180, 1997.

Pereda A, Triller A, Korn H, Faber DS. Dopamine enhances both electrotonic coupling and chemical excitatory postsynaptic potentials at mixed synapses. *Proc Natl Acad Sci USA* 89: 12088–12092, 1992.

Pereda AE, Nairn AC, Wolszon LR, Faber DS. Postsynaptic modulation of synaptic efficacy at mixed synapses on the Mauthner cell. *J Neurosci* 14: 3704–3712, 1994.

Prescott SA, De Koninck Y. Gain control of firing rate by shunting inhibition: roles of synaptic noise and dendritic saturation. *Proc Natl Acad Sci USA* 100: 2076–2081, 2003.

Preuss T, Faber DS. Central cellular mechanisms underlying temperature-dependent changes in the goldfish startle-escape behavior. *J Neurosci* 23: 5617–5626, 2003.

Preuss T, Osei-Bonsu PE, Weiss SA, Wang C, Faber DS. Neural representation of object approach in a decision-making motor circuit. *J Neurosci* 26: 3454–3464, 2006.

Pruden AJ, Uetz GW. Assessment of potential predation costs of male decoration and courtship display in wolf spiders using video digitization and playback. *J Insect Behav* 17: 67–80, 2004.

Renn SC, Aubin-Horth N, Hofmann HA. Fish and chips: functional genomics of social plasticity in an African cichlid fish. *J Exp Biol* 211: 3041–3056, 2008.

Ripley JL, Lobel PS, Yan HY. Correlation of sound production with hearing sensitivity in the Lake Malawi cichlid, *Tramitachromis intermedius.* *Bioacoustics* 12: 238–240, 2002.

Ritter DA, Bhatt DH, Fetcho JR. In vivo imaging of zebrafish reveals differences in the spinal networks for escape and swimming movements. *J Neurosci* 21: 8956–8965, 2001.

Robinson GE, Fernald RD, Clayton DF. Genes and social behavior. *Science* 322: 896–900, 2008.

Schlegel T, Schuster S. Small circuits for large tasks: high-speed decision-making in archerfish. *Science* 319: 104–106, 2008.

Spitzer N, Antonsen BL, Edwards DH. Immunocytochemical mapping and quantification of expression of a putative type 1 serotonin receptor in the crayfish nervous system. *J Comp Neurol* 484: 261–282, 2005.

Sur C, Korn H, Triller A. Colocalization of somatostatin with GABA or glutamate in distinct afferent terminals presynaptic to the Mauthner cell. *J Neurosci* 14: 576–589, 1994.

Szabo TM, Brookings T, Preuss T, Faber DS. Effects of temperature acclimation on a central neural circuit and its behavioral output. *J Neurophysiol* 100: 2997–3008, 2008.

Szabo TM, Weiss SA, Faber DS, Preuss T. Representation of auditory signals in the M-cell: role of electrical synapses. *J Neurophysiol* 95: 2617–2629, 2006.

Trainor BC, Hofmann HA. Somatostatin regulates aggressive behavior in an African cichlid fish. *Endocrinology* 147: 5119–5125, 2006.

Trainor BC, Hofmann HA. Somatostatin and somatostatin receptor gene expression in dominant and subordinate males of an African cichlid fish. *Behav Brain Res* 179: 314–320, 2007.

Verzijden MN, van Heusdena J, Boutona N, Witte F, ten Cate C, Slabbekoorn H. Sounds of male Lake Victoria cichlids vary within and between species and affect female mate preferences. *Behav Ecol* 21: 548–555, 2010.

Vu ET, Berkowitz A, Krasne FB. Postexcitatory inhibition of the crayfish lateral giant neuron: a mechanism for sensory temporal filtering. *J Neurosci* 17: 8867–8879, 1997.

Weiss SA, Preuss T, Faber DS. A role of electrical inhibition in sensorimotor integration. *Proc Natl Acad Sci USA* 105: 18047–18052, 2008.

Weiss SA, Preuss T, Faber DS. Phase encoding in the Mauthner system: implications in left-right sound source discrimination. *J Neurosci* 29: 3431–3441, 2009.

Weiss SA, Zottoli SJ, Do SC, Faber DS, Preuss T. Correlation of C-start behaviors with neural activity recorded from the hindbrain in free-swimming goldfish, Carassius auratus. *J Exp Biol* 209: 4788–4801, 2006.

Winberg S, Winberg Y, Fernald RD. Effect of social rank on brain monoaminergic activity in a cichlid fish. *Brain Behav Evol* 49: 230–236, 1997.

Wong RY, Hofmann HA. Behavioural genomics: An organismic perspective. In: *Encyclopedia of Life Sciences* (ELS). Chichester: Wiley & Sons, 2010.

Ydenberg RC, Dill LM. The economics of fleeing from predators. *Adv Stud Behav* 16: 229–249, 1986.

Yeh SR, Fricke RA, Edwards DH. The effect of social experience on serotonergic modulation of the escape circuit of crayfish. *Science* 271: 366–369, 1996.

Yeh SR, Musolf BE, Edwards DH. Neuronal adaptations to changes in the social dominance status of crayfish. *J Neurosci* 17: 697–708, 1997.

Zottoli SJ. Correlation of the startle reflex and Mauthner cell auditory responses in unrestrained goldfish. *J Exp Biol* 66: 243–254, 1977.

Zottoli SJ, Marek LE, Agostini MA, Strittmatter SL. Morphological and physiological survival of goldfish Mauthner axons isolated from their somata by spinal-cord crush. *J Comp Neurol* 255: 272–282, 1987.

Zottoli SJ, Newman BC, Rieff HI, Winters DC. Decrease in occurrence of fast startle responses after selective Mauthner cell ablation in goldfish, Carassius auratus. *J Comp Physiol [A]* 184: 207–218, 1999.